NUMERICAL INVESTIGATION OF CONDENSATION INSIDE AN INCLINED SMOOTH TUBE

Noori Rahim Abadi S. M. A., Meyer J.P.*, and J. Dirker
*Author for correspondence
Department of Mechanical and Aeronautical Engineering,
University of Pretoria,
Pretoria, 0002,
South Africa,
E-mail: josua.meyer@up.ac.za

ABSTRACT

In this paper the effect of inclination angle on the condensation heat transfer coefficient, pressure drop and flow regime inside a smooth tube was investigated numerically. The working fluid was R134a at a saturation temperature of 40°C. The Volume of Fluid (VOF) multiphase flow formulation was utilized to solve the governing equations. Simulations were conducted at a heat flux of 5 kW/m^2, at mass fluxes of 100 – 600 kg/m^2.s, and the inclination angles were varied from vertical downward to vertical upward. The simulation results were successfully validated with the experimental data. The results showed that an optimum downward inclination angle of between -30° and -15° exists, for the heat transfer coefficients. It was also found that the effect of inclination angle on the pressure drop and void fraction became negligible at high mass fluxes and vapour qualities.

INTRODUCTION

Condensation inside tubes can be found in the air-conditioning, refrigeration, automotive, power generation and chemical processing industries. For design and optimization purposes, a deep understanding is required of the phenomena of flow patterns, heat transfer coefficients and pressure drops during condensation [1-5].

Many applications involve condensation inside inclined tubes usually constructed in an A-frame structure for dry-cooled steam condensers and in some rooftop industrial air-cooled refrigeration systems. Literature reviews show that previous works on the condensation phenomenon in inclined tube are very limited. This has been confirmed by Lips and Meyer [6] who performed a comprehensive literature review of the effect of the inclination angle on the condensation inside smooth tubes. They showed that little experimental data exist and despite numerous studies, that no generalized method for the prediction of two-phase flow has been widely accepted in the literature.

Lips and Meyer [7-9] studied the effect of the tilt angle on the condensation inside a smooth tube experimentally. Their investigations led to a better understanding of the condensation phenomenon in inclined tubes. They used a smooth circular tube with an inside diameter of 8.38 mm and a length of 1.488 m. The working fluid was R134a and the saturation temperature was fixed at 40°C. The authors studied the effect of tube orientation on pressure drop, void fraction and heat transfer coefficient. Furthermore, they generated several flow-map patterns at different inclination angles from visual observations.

Del Col et al. [10] studied the condensation phenomenon inside inclined square cross sectional mini channels with a diameter of 1.32 mm experimentally. They used two refrigerants, R134a and R32, and the saturation temperature was fixed at 40 0C. They found that the orientation of the channel had a negligible effect on condensation when flow occurs in a downward direction at high mass fluxes. However, for upward flow the effects were not only limited to high mass fluxes, but were observed for all mass fluxes. Also for downward flow the inclination angle had a significant effect on the heat transfer coefficients at vapour qualities less than about 0.6 and mass fluxes lower than the critical values for both refrigerants.

NOMENCLATURE

F	[N/m^3]	Source term in the momentum equation
g	[m/s^2]	Gravitational acceleration
h	[W/m^2.K]	Heat transfer coefficient
h	[j/kg]	Enthalpy
k	]m^2/s^2]	turbulent kinetic energy
P	[Pa]	Pressure
q''	[W/m^2]	Heat flux
S	[kg/m^3.s]	Source term
t	[s]	Time
T	[K]	Temperature
T_{sat}	[K]	Saturation temperature
u	[m/s]	Velocity
x	[m]	Distance in horizontal direction
y	[m]	Distance in vertical direction

Special characters

α	[-]	Volume fraction
μ	[Pa.s]	Molecular viscosity
τ	[N/m^2]	Shear tension
ρ	[kg/m^3]	Density
k	[-]	Curvatures of liquid and vapor phase
ε	[m^2/s^3]	Turbulent dissipation rate
β	[Deg]	Inclination angle
σ	[N/m]	Surface tension

Subscripts

ave	Average
l	Liquid
v	Vapour

Del Col et al developed a method to predict at which mass flux the channel inclination starts to affect the condensation heat transfer by using the Buckingham theorem.

Work were done to study the effect of inclination angle in the presence of non-condensable gases [11-12]. Caruso and Mio [13] investigated the steam condensation in presence of non-condensable gases within horizontal and inclined tubes theoretically and experimentally. Their results showed that the presence of non-condensable gases adversely affect the condensation efficiency and heat transfer. They also presented a simple correlation based on dimensionless numbers and compared the results with previous formulations.

Literature reviews therefore show that all the previous studies regarding condensation in inclined tube were mainly conducted experimentally [14-15] and some using an analytical approach [16-17] with many simplifying assumptions. Computational Fluid Dynamics (CFD) of condensation phenomenon inside inclined tube can explain the flow characteristics inside the tube with the minimum cost and time, however, no such studies have been conducted. In this study, numerical simulations were performed to investigate the effect of inclination angle on the void fraction, pressure drop and heat transfer along a smooth tube at different inclination angles.

GOVERNING EQUATIONS

In this study the well-known Volume of Fluid (VOF) multiphase flow formulation [18] is used for the simulation of the condensation phenomenon inside the inclined tube.

The continuity equations for the volume fractions of each phase are presented as follows:

$$\frac{\partial \alpha_v}{\partial t} + \nabla.(u\alpha_v) = \frac{S_v}{\rho_v} \tag{1}$$

$$\frac{\partial \alpha_l}{\partial t} + \nabla.(u\alpha_l) = \frac{S_l}{\rho_l} \tag{2}$$

Where u and t are velocity and time respectively. Parameter S is the source term due to phase change.

As the velocity difference between each phase is neglected in the VOF method only one momentum equation is presented as follows:

$$\begin{aligned} &\frac{\partial(\rho_m u)}{\partial t} + \nabla.(\rho_m uu) = -\nabla p \\ &+\nabla.[\mu_{m,eff}(\nabla u + (\nabla u)^T) - \frac{2}{3}\mu_{m,eff}\nabla.uI] \\ &+\rho_m g + F_\sigma + S_u \end{aligned} \tag{3}$$

Where ρ, p, g and F_σ are density, pressure, gravitational acceleration and surface tension force respectively. The parameter I is the 3×3 identity matrix. The energy equation is also defined as:

$$\frac{\partial(\rho_m E)}{\partial t} + \nabla.[u(\rho_m E + p)] = \nabla.(k_{m,eff}\nabla T) + S_E \tag{4}$$

Where E and k are internal energy and thermal conductivity respectively.

The surface tension force is computed by the CSF model for the cells containing the vapour-liquid interface [19]. The continuum surface force (CSF) model has been implemented such that the addition of surface tension to the VOF calculation results in a source term in the momentum equation as follows:

$$F_\sigma = \sigma \frac{\alpha_l \rho_l k_v \nabla \alpha_v + \alpha_v \rho_v k_l \nabla \alpha_l}{\frac{1}{2}(\rho_v + \rho_l)} \tag{5}$$

Where σ is the water surface tension. The curvatures of the liquid and vapour phase are defined as:

$$k_l = \frac{\Delta \alpha_l}{|\nabla \alpha_l|}, \quad k_v = \frac{\Delta \alpha_v}{|\nabla \alpha_v|} \tag{6}$$

In this study the two-equation turbulence model, realizable k- , is applied. The equations of turbulence energy and dissipation rate are represented as follows:

$$\begin{aligned} &\frac{\partial(\rho_m k)}{\partial t} + \frac{\partial(\rho_m u_j k)}{\partial x_j} = \frac{\partial}{\partial x_j}[(\mu_{m,L} + \frac{\mu_{m,T}}{\sigma_k})\frac{\partial k}{\partial x_j}] \\ &+\tau_{ij}\frac{\partial u_i}{\partial x_j} + \beta g \frac{\mu_{m,T}}{\sigma_k}\frac{\partial T}{\partial y} - \rho_m \varepsilon \end{aligned} \tag{7}$$

$$\begin{aligned} &\frac{\partial(\rho_m \varepsilon)}{\partial t} + \frac{\partial(\rho_m u_j \varepsilon)}{\partial x_j} = \frac{\partial}{\partial x_j}(\frac{\mu_{m,T}}{\sigma_\varepsilon}\frac{\partial \varepsilon}{\partial x_j}) + pC_1 S\varepsilon \\ &-\rho_m C_{2\varepsilon}\frac{\varepsilon^2}{k + \sqrt{v\varepsilon}} + C_{1\varepsilon}\frac{\varepsilon}{k}C_{3\varepsilon}\beta g \frac{\mu_{m,T}}{\sigma_\varepsilon}\frac{\partial T}{\partial y} \end{aligned} \tag{8}$$

Where:

$$C_1 = \max[0.43, \frac{\eta}{\eta + 5}], \ \eta = S\frac{k}{\varepsilon}, \ S = \sqrt{2S_{ij}S_{ij}} \tag{9}$$

The stress tensor (τ_{ij}) for each phase is defined as follows:

$$\tau_{ij} = (\mu_{m,L} + \mu_{m,T})(\frac{\partial u_i}{\partial x_j} + \frac{\partial u_i}{\partial x_j} - \frac{2}{3}\frac{\partial u_j}{\partial x_j}\delta_{ij}) - \frac{2}{3}\rho_m k\delta_{ij} \tag{10}$$

Turbulent viscosity (μ_T) relates turbulence energy (k) and dissipation rate (ε) such that:

$$\mu_{m,T} = C_\mu \frac{\rho_m k^2}{\varepsilon} \tag{11}$$

Where C_μ is a function of the mean strain and rotation rates, the angular velocity of the system rotation, and the turbulence fields. The empirical constants used in the turbulence model are summarized below:

$$\begin{aligned} &C_{1\varepsilon} = 1.44, \ C_{2\varepsilon} = 1.92 \\ &C_{3\varepsilon} = \tanh\left|\frac{v}{u}\right|, \ \sigma_k = 1.0, \ \sigma_\varepsilon = 1.3 \end{aligned} \tag{12}$$

Details of the various parameters used in the turbulence model are given in ref. [20].

In this study the effect of phase phenomenon is considered via source terms in the governing equations. The condensation source terms can be expressed as in ref. [21, 22]:

$$S_l = r_l \alpha_l \rho_l \frac{T - T_{sat}}{T_{sat}} \quad T \geq T_{sat} \tag{13}$$

$$S_v = r_v \alpha_v \rho_v \frac{T_{sat} - T}{T_{sat}} \quad T < T_{sat} \tag{14}$$

where T_{sat} is the saturation temperature of the working fluid. The coefficients r_1 and r_2 should be tuned such to fit the model to experimental data. Excessively small values of the coefficient r lead to a significant deviation between the interfacial and saturation temperature. However, too large values of r cause numerical convergence problems. In the present study the value of r_l and r_v were considered to be 1 500 s^{-1} [23].

The relevant source terms in momentum and energy equations are defined as follows:

$$S_{uj} = Su_j$$
$$S_E = Sh_{lv} \tag{15}$$

Where h_{lv} is a latent heat of condensation. The aforementioned source terms in mass, momentum and energy equations were implemented in the solver via User Defined Function (*UDF*).

The average heat transfer coefficient along the tube was also calculated as follows:

$$h_{ave} = \frac{q''}{T_{sat} - T_{wall,ave}} \tag{16}$$

Where the $T_{wall,\ ave}$ and q'' are the average tube wall temperature and heat flux respectively.

The following assumptions were made for the simulations:

1. The flow regimes are slug or annular. Therefore, it is always possible to capture a certain two-phase interface.
2. The flow field is considered to be three-dimensional, unsteady and turbulent.
3. The velocity difference between liquid and vapour phases is neglected.
4. The properties of each phases is assumed to be constant at the specified operating condition.
5. The interface temperature is assumed to be at the saturation temperature.

Figure 1 shows the computational domain of the present numerical study. The computational domain is a 8.38 mm diameter circular smooth tube with a length of 1.488 m. The following boundary conditions were assumed for all simulations:

1. Inlet: At the inlet section of the domain, the mass fluxes of vapour and liquid phases and mixture temperature are given.
2. Outlet: At the outlet section only the static gauge pressure of 0 Pa is given.
3. Walls: The constant heat flux of 200 W and no slip condition are assumed at the tube wall. The contact angle between liquid and solid at saturation temperature of 40 °C is set to 5.8° [24].

Furthermore, the whole volume of the tube was considered to be vapour with the constant temperature equal to the saturation temperature as the initial condition.

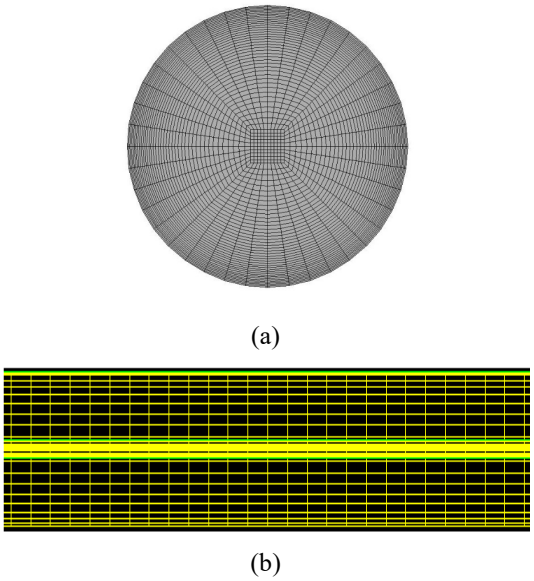

(a)

(b)

Figure 1 The computational domain; (a) tube cross section, (b) close-up of tube side view in the axial flow direction.

To solve the governing equations the ANSYS FLUENT 17.1 commercial software package was utilized. The pressure-velocity coupling was achieved by using a two-phase extension of the well-known SIMPLE algorithm. To obtain a stable solution procedure, all the convective fluxes were approximated by a second-order upwind method while the diffusive fluxes were discretized by central differencing. To capture the liquid/vapour interphase the Geo-Reconstruction scheme was utilized. The convergence criterion was set to 10^{-5} for the residual of each parameter. A time-step size of 10^{-4} s was used for the simulations.

RESULTS AND DISCUSSION

Various operating conditions were considered in this study. The refrigerant mass flux, G, varied between 100 - 400 kg/m^2.s and the inclination angle, $ß$, was varied from -90° (vertical downward flow) to +90° (vertical upward flow). The mean vapour mass fraction, x_m, was varied from 0.1 – 0.9. All simulations were conducted at a saturation temperature of 40°C. A grid dependency study was conducted with grid sixes varying between 360 000 to 1 640 000 cells were conducted. A grid size of 960 000 was selected as it was found to be a good compromise between grid size independent results, accuracy, and simulation time.

Figure 2 shows the variations of heat transfer coefficients as function of inclination angle for different values of vapour mass fractions. The agreements between numerical results and experimental results are good, with the biggest deviations occurring at lower inclination angles.

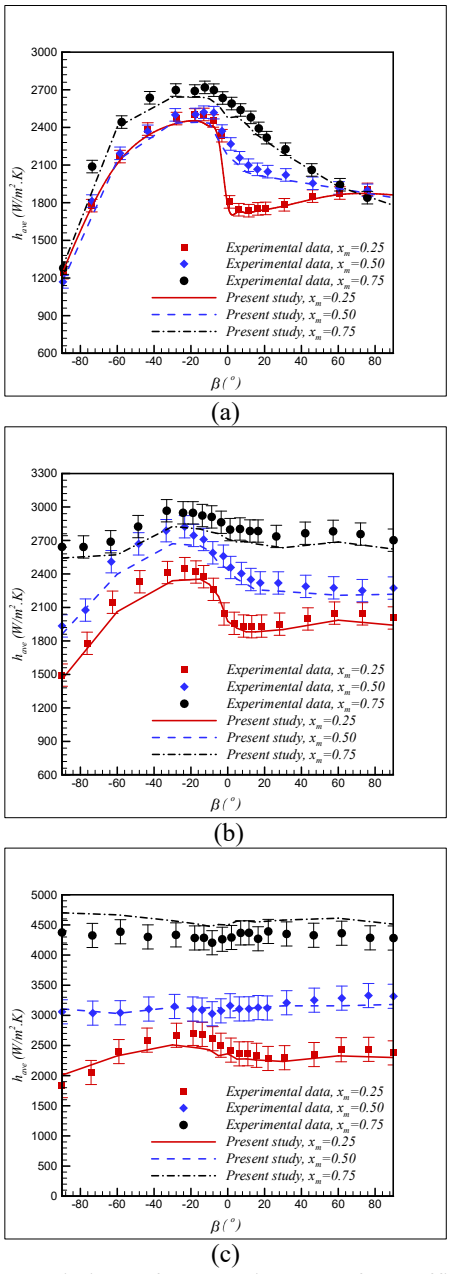

Figure 2 Variations of average heat transfer coefficient as function of inclination angle for different values of vapour mass flux; (a) G=100 kg/m^2.s, (b) G=200 kg/m^2.s and (c) G=300 kg/m^2.s

The heat transfer coefficients increased with a decrease of the inclination angle from -90° to approximately -30°. Such trend is more significant at lower volume fractions and refrigerant mass fluxes. As the downward inclination angle increase the thermal resistance decreases as a result of flowing liquid film in the direction of the flow. As the tube inclination angle further decreases to reach the β=10°-20°, the heat transfer coefficient decreases due to change in the flow regime and breakup of liquid film, which results in an increase of the thermal resistance. At higher refrigerant mass fluxes the flow regimes did not change significantly (almost annular with relative constant liquid thickness), therefore, there was a liquid film on the tube wall.

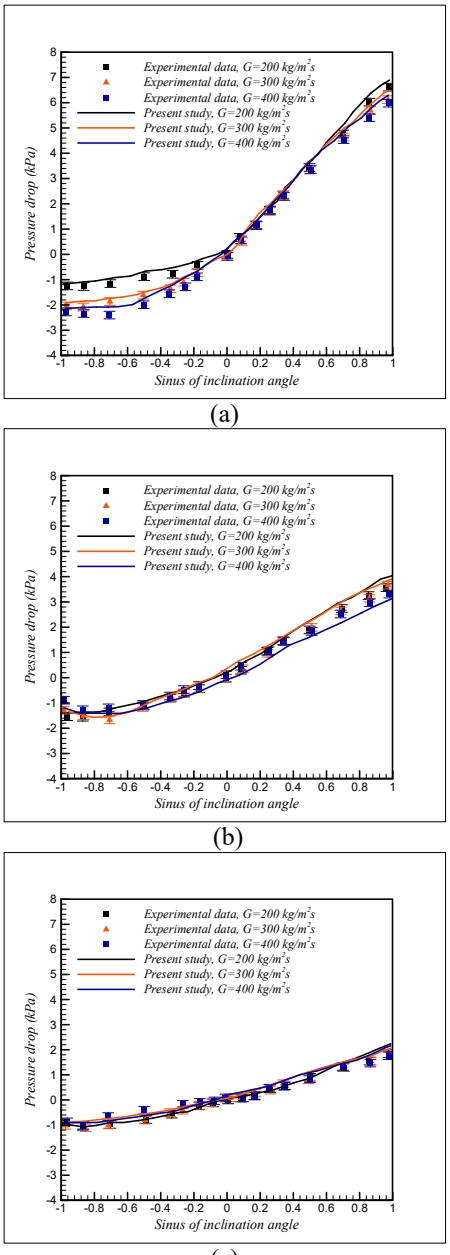

Figure 3 Variations of pressure drop as function of inclination angle for different values of vapour mass fraction; (a) x_m=0.25, (b) x_m=0.5, (c) x_m=0.75.

With an increase of vapour mass fraction the heat transfer coefficients increased significantly. It is due to the fact that at higher vapour mass fractions the liquid film in the tube decreased, which resulted in a decrease in the thermal resistance. It was also found that the tube inclination angle had a negligible effect on the heat transfer coefficient when the vapour mass fraction increased within the tube.

Figure 3 shows the variations of pressure drop along the tube at different inclination angles, vapour mass fractions and refrigerant mass fluxes. The predicted results show very good agreements with experimental data. However, at higher mass flow rates the deviations are a more than for lower mass fluxes. As can be seen in **Figure 3**, the pressure drop along the tube increases with the changes in the inclination angle from $\beta = -90°$ to $\beta = +90°$. It is mainly because of gravity which acts in the opposite direction when the orientation gradually tends to vertical upward directions. Furthermore, the plots show that the inclination angle has a much more significant effect on the pressure drop when the flow direction is upward. It is because the flow regime in an upward direction is mostly annular, therefore the shear forces are dominant and the gravity forces has a negligible effect. Also, shown in the graph is that with an increase of vapour mass fraction the pressure drop decreased significantly. It is because larger values of vapour mass fraction lead to a decrease of mixture density.

Figure 4 shows the numerically simulated and measured void fractions as function of inclination angles. In general, the predicted values are in good agreement with experimental data, which proves the capability of the presented numerical method to accurately predict the condensation phenomenon inside inclined smooth tubes during condensation. The results in **Figure 4** show that the values of the void fractions increase with an increase of vapour quality.

For a mass flux of 100 kg/m^2.s, and for upward flow, the void fraction values for a quality of 25%, decreased significantly. It is because at low mass fluxes when the flow direction turned upward the flow regime changed from stratified-wavy to churn, which decreased the void fractions values. When the qualities increased to 50%, and 75%, the flow regimes remained stratified or stratified-wavy, therefore, the inclination angle had no significant effect on the void fractions.

At a mass flux of 200 kg/m^2.s, the results compared well with the measurements, however, the results are less dependent on quality. Furthermore, effects of the inclination angles on void fractions were less significant. The reason is that as the mass fluxes increases the shear forces increases while the gravity forces remains constant. The flow regimes therefore remain annular or stratified. This tendency of the void fraction becoming independent of inclination angle as the mass flux increased is best illustrated by comparing the void fractions at a mass flux of 300 kg/m^2.s, with the void fractions at mass fluxes of 200 kg/m^2.s, and 100 kg/m^2.s.

Figures 5 and 6 show the contours of volume fraction for G=100 kg/m^2.s at two values of the vapour volume fractions, $x_m = 0.25$ and $x_m = 0.75$, at different inclination angles. As discussed previously, at low refrigerant mass fluxes and vapour volume fractions when the flow direction changes upwards the flow regime changes from annular or stratified to churn.

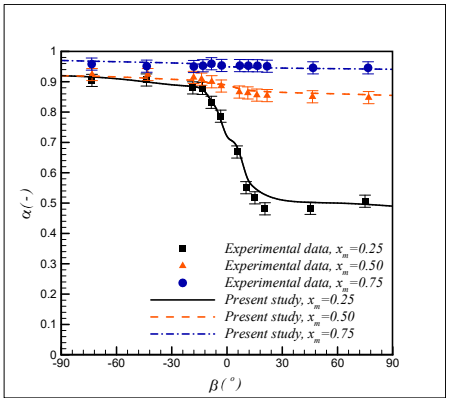

(a)

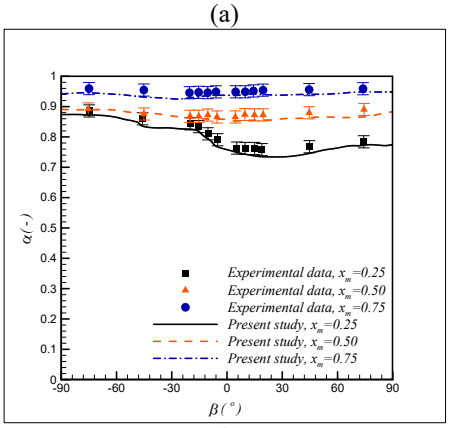

(b)

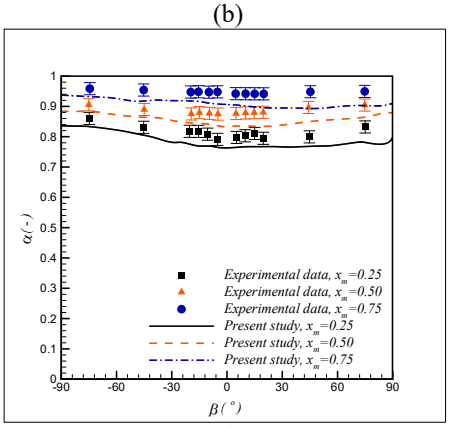

(c)

Figure 4 Variations of void fraction as function of inclination angle for different values of vapour mass fraction; (a) G=100 kg/m^2.s, (b) G=200 kg/m^2.s and (c) G=300 kg/m^2.s.

With a further increase of vapour volume fraction the shear force surpasses the gravity force and causes the flow regime to remain annular or stratified (**Figures 6 (a) to (g)**).

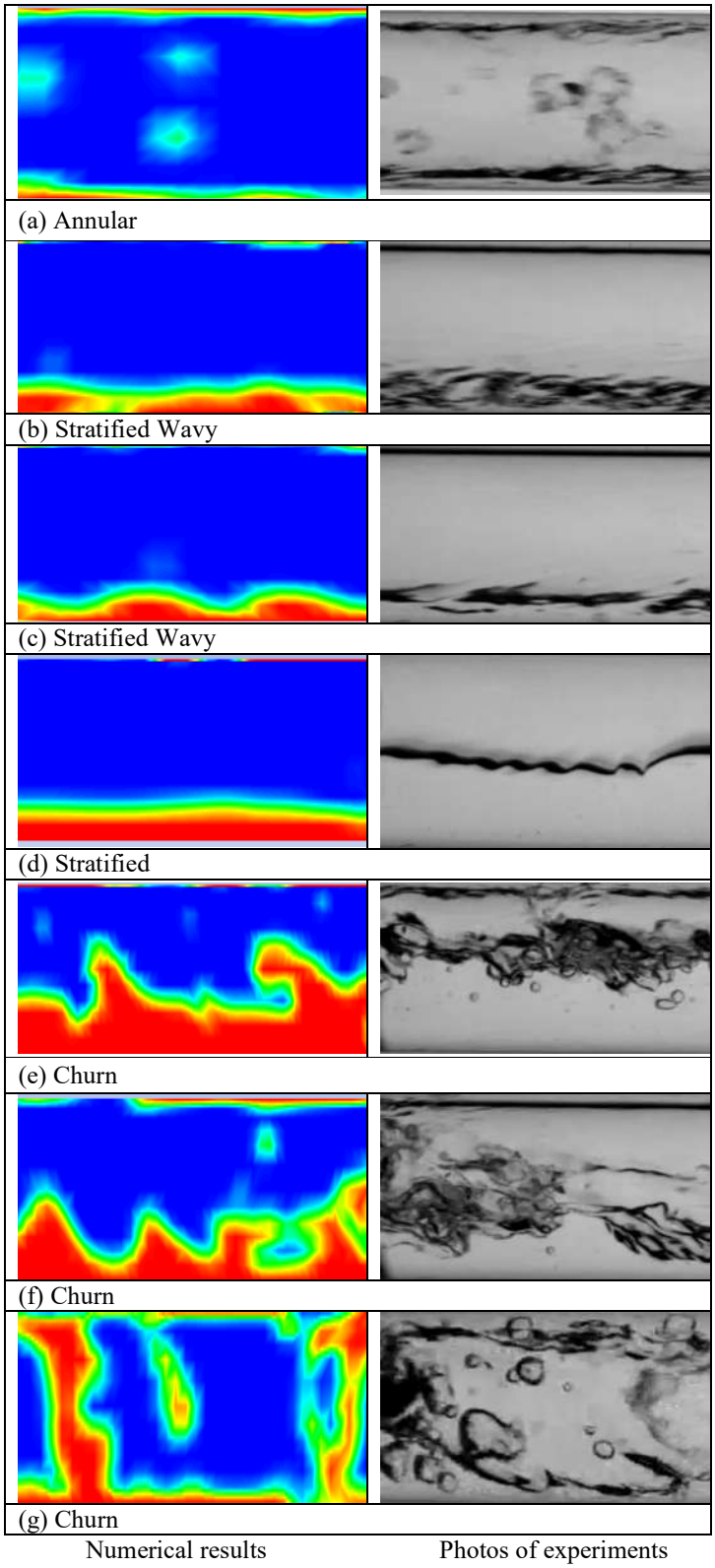

Figure 5 Contours of volume fraction for $x_m = 0.25$ and $G = 100$ kg/m^2.s at different tube inclination angles; (a) θ = -90°, (b) θ = -60°, (c) θ = -30°, (d) θ = 0°, (e) θ = +30°, (f) θ = +60°, (g) θ = +90°.

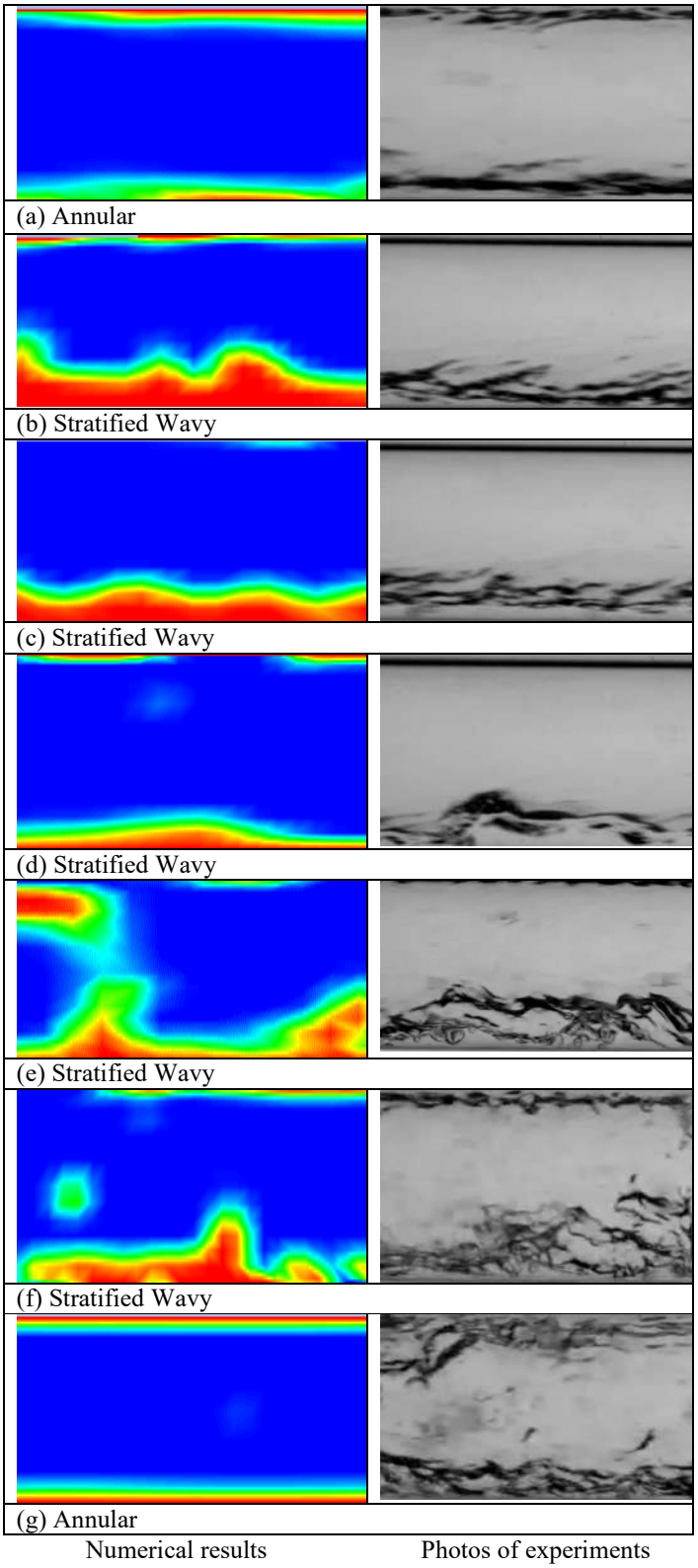

Figure 6 Contours of volume fraction for $x_m = 0.75$ and $G = 100$ kg/m^2.s at different tube inclination angles; (a) θ = -90°, (b) θ = -60°, (c) θ = -30°, (d) θ = 0°, (e) θ = +30°, (f) θ = +60°, (g) θ = +90°.

CONCLUSION

In this paper the effect of inclination angle, refrigerant mass flow rate and vapour volume fraction on the void fraction and pressure drop, heat transfer coefficient and flow regime inside a smooth tube was investigated numerically. The governing equations were applied using the VOF multiphase flow method. The flow field was assumed to be unsteady, turbulent and three dimensional. Furthermore, the fluids properties were considered to be constant as temperature changes were negligible. The Volume of Fluid (VOF) multiphase flow formulation was applied and the ANSYS FLUENT 17.1 commercial software package was utilized to numerically solve the governing equations. The following conclusions were made:

I. The effect of inclination angle became negligible at high refrigerant mass flow rates and vapour mass fractions.
II. With an increase of void fraction the pressure drop along the tube increased.
III. The pressure drop increased as the refrigerant mass flux increased.
IV. At low vapour mass fractions or refrigerant mass fluxes, the change in flow direction from downward to upward leads to a change in the flow regime from annular or stratified to churn. This resulted in a decrease in the void fraction and an increase in the pressure drop.
V. An optimum inclination angle region between -30° and -15° exists in which the heat transfer coefficient reaches its maximum.

REFERENCES

[1] Liebenberg, L., Meyer, J. P., A review of flow pattern-based predictive correlations during refrigerant condensation in horizontally smooth and enhanced tubes, *Heat Transfer Engineering*, Vol. 29, 2008, pp. 3-19.

[2] Cavallini, A., Brown, J. S., Del Col, D., Zilio, C., In-tube condensation performance of refrigerants considering penalization terms (energy losses) for heat transfer and pressure drop, *International Journal of Heat and Mass Transfer*, Vol. 53, 2010, pp. 2885-2896.

[3] Ould Didi, M. B., Kattan, N., Thome, J. R., Prediction of two-phase pressure gradients of refrigerants in horizontal tubes, *International Journal of Refrigeration*, Vol. 25, 2002, pp. 935-947.

[4] Miyara, A., Condensation of hydrocarbons – a review, *International Journal of Refrigeration*, Vol. 31, 2008, pp. 621-632.

[5] Dalkilic, A. S., Wongwise, S., Intensive literature review of condensation inside smooth and enhanced tubes, *International Journal of Heat and Mass Transfer,* Vol. 52, 2009, pp. 3409-3426.

[6] Lips, S., Meyer, J. P., Two-phase flow in inclined tubes with specific reference to condensation: A review, *International Journal of Multiphase Flow*, Vol. 37, 2011, pp. 845-859.

[7] Lips, S., Meyer, J. P., Experimental study of convective condensation in an inclined smooth tube. Part I: Inclination effect on flow pattern and heat transfer coefficient, *International Journal of Heat and Mass Transfer*, Vol. 55, 2012, pp. 395-404.

[8] Lips, S., Meyer, J. P., Experimental study of convective condensation in an inclined smooth tube. Part II: Inclination effect on pressure drops and void fractions, *International Journal of Heat and Mass Transfer*, Vol. 55, 2012, pp. 405-412.

[9] Lips, S., Meyer, J. P., Effect of Gravity Forces on Heat Transfer and Pressure Drop During Condensation of R134a, *Microgravity Science Technology*, Vol. 24, 2012, pp. 157-164.

[10] Del Col, D., Bortolato, M., Azzolin, M., Bortolin, S., Effect of inclination during condensation inside a square cross section minichannel, *International Journal of Heat and Mass Transfer*, Vol. 78, 2014, pp. 760-777.

[11] Caruso, G., Maio, D. V., Naviglio, A., Film condensation in inclined tubes with noncondensable gases: an experimental study on the local heat transfer coefficient, *International communication in Heat and Mass Transfer*, Vol. 45, 2013, pp.1-10.

[12] Caruso G., Giannetti, F., Naviglio, A., Experimental investigation on pure steam and steam-air mixture condensation inside tubes, *International Journal of Heat and Technology*, Vol. 30, 2012, pp. 77-84.

[13] Caruso, G., Maio, D. V., Heat and mass transfer analogy applied to condensation in the presence of non-condensable gases inside inclined tubes, *International Journal of Heat and Mass Transfer*, Vol. 68, 2014, pp. 401-414.

[14] Caruso, G., Vitale di Maio, D., Naviglio, A., Condensation heat transfer coefficient with noncondensable gases inside near horizontal tubes, *Desalination*, Vol. 309, 2013, pp. 247-253.

[15] Chato, J. C., Laminar condensation inside horizontal and inclined tubes, *American Society Heating Refrigerating Air Conditioning Engineering (ASHRAE) Journal*, Vol. 4, 1962, pp. 52-60.

[16] Beggs, D. H., Brill, J. P., A study of two-phase flow in inclined pipes, *Journal of Petroleum Technology*, Vol. 25, 1973.

[17] Lips, S., Meyer, J. P., Stratified flow model for convective condensation in an inclined tube, *International Journal of Heat and Fluid Flow*, Vol. 36, 2012, pp. 83-91.

[18] Hirt, C. W., Nichols, B. D., Volume of fluid (VOF) method for the dynamics of free boundaries. *Journal of Computational Physics*, Vol. 39, 1981, pp.201-225.

[19] Brackbill, J. U., Kothe, D. B., Zemach, C., A Continuum Method for Modeling Surface Tension, *Journal of Computational Physics*, Vol. 100, 1992, pp. 335-354.

[20] Yang, Z., Shih, T. H., New time scale based k- model for near wall turbulence. *AIAA Journal*, Vol. 317, 1993, pp. 1191-1197.

[21] Lee, W. H., A Pressure Iteration Scheme for Two-Phase Flow Modeling, Multiphase Transport: Fundamentals, Reactor Safety, Applications, Verizoglu, T. N. ed., Hemisphere Publishing, Washington, DC, 1980.

[22] Liu, Z., Sunden, B., Yuan, J., VOF Modeling and analysis of Film wise condensation between vertical parallel plates, *Heat Transfer Research*, Vol. 43, 2012, pp. 47-68.

[23] Lee, W. H., A pressure iteration scheme for two-phase modeling. Technical Report LA-UR 79-975, Los Alamos Scientific Laboratory, Los Alamos, New Mexico, 1979.

[24] Vadgama, B., Harris, D. K., Measurements of the contact angle between R134a and both aluminium and copper surfaces, *Experimental Thermal and Fluid Science*, Vol. 31, 2007, pp. 979-984.